LAAS Study of Slow-Moving Ionosphere Anomalies and Their Potential Impacts

Ming Luo, Sam Pullen, Seebany Datta-Barua, Godwin Zhang, Todd Walter, and Per Enge

Stanford University

ABSTRACT

Triggered by several severe ionosphere storms that have occurred in recent years, research has been done to studying those anomalies, the physics behind them, and their potential impact on augmented GNSS users. In previous work [1-5], it was found that such ionosphere anomalies can threaten LAAS users under extreme conditions. To determine this, a spatial-gradient "threat model" was established based on ionosphere storm data observed from WAAS and IGS since 2000. Maximum differential user vertical errors were estimated based on this threat model. Although LGF monitors can detect "moving fronts", so-called "stationary fronts" remain threatening since the LGF may never be able to observe it (e.g., if the ionosphere front stops moving at the worst possible location prior to reaching the LGF).

In order to validate the threat model, a comprehensive methodology was developed to analyze WAAS "supertruth" data as well as both raw and JPL-processed data from the IGS/CORS receiver network to search for anomalous gradients [15]. Anomalous gradients that result from this method were used to populate and validate the LAAS ionosphere spatial gradient "threat model". These data studies show that most of the ionosphere anomalies seem to move reasonably fast relative to the speed of an approaching aircraft. The few data points thought to be stationary were impossible to validate after a thorough investigation. Additional data analysis has been performed to better determine the credibility of the slow-moving segment of the ionosphere spatial anomaly threat space.

In this paper, data from the Ohio/Michigan cluster of CORS stations on November 20, 2003 and from the Florida region on October 31, 2003 (UTC) are searched for slow-moving ionosphere events. One data point that stood out was verified by observation at various locations using both the dual-frequency JPL data as well as L1 code-minus-carrier estimation. A threat analysis follows to show the potential impact of this observed threat under various GPS constellation states. A sensitivity study is conducted to show how the impact relies on the upper bound of the slow-moving threat model. A "data replay" analysis is also performed to show the actual LAAS errors that would have occurred at one pair of stations in Florida. Finally, a recommendation is made in for revising the upper bound of the slow-moving threat space.

1.0 INTRODUCTION

The ionosphere is a dispersive medium located in the region of the upper atmosphere between about 50 km to about 1000 km above the Earth [6]. The radiation of the Sun produces free electrons and ions that cause phase advance and group delay in radio waves. The state of the ionosphere is a function of the intensity of solar activity, magnetic latitude, local time, and other factors. As GPS signals traverse the ionosphere, they are delayed by an amount proportional to the Total Electron Content (TEC) within the ionosphere at a given time. Because the ionosphere is constantly changing, the error introduced by the ionosphere into the GPS signal is highly variable and is difficult to model at the level of precision needed for LAAS. However, under nominal conditions, the spatial gradient is in the range of 2 – 5 mm/km (1σ); thus typical LAAS user errors are small (less than 10 cm, 1σ).

The possibility of extremely large ionosphere spatial gradients was originally discovered in the study of WAAS "supertruth" (post-processed, bias-corrected) data during ionosphere storm events at the time of the last solar maximum (2000 – 2001). It was estimated that an ionosphere storm on 6 April 2000 resulted in a 7 m differential delay over the IPP separation of 19 km. This translates into an ionosphere delay rate of change of approximately 316 mm/km, which is two orders of magnitude higher than the typical one-sigma ionosphere vertical gradient value identified previously. Since a Gaussian extrapolation of the 5 mm/km one-sigma number planned to be broadcast by the LAAS Ground Facility (LGF) does not come close to overbounding this extreme gradient, and because it is impractical to dramatically increase the broadcast one-sigma number without losing all system availability, we must treat this event as an anomaly and detect and exclude cases of it that lead to hazardous user errors. The detailed study on the 6 April 2000 storm can be found in [1].

Several ionosphere storms of concern have occurred since the April 2000 storm. Among them, the two largest ones were on October 29-31, 2003 and November 20, 2003. Figure 1 shows a snapshot of the ionosphere delay map over CONUS on October 29, 2003 between 20:00 to 20:45 in UTC time. The subplots are "snapshots" taken 15 minutes apart. The *x*-axis and *y*-axis represent longitude and latitude, respectively. The color scale indicates the magnitude of the vertical ionosphere delay.

Dark red represents about 20 meters of delay, and dark blue represents about 2 meters. As can be seen, there are some sharp transitions between the dark red and the blue, which indicates sharp spatial gradients in those areas. By comparing the subplots, it appears that the storm did not move much during the 45 minutes covered by the subplots. An ionosphere movie made during that period (with finer time resolution) also indicates that the anomaly may have been "near stationary" at specific locations and times. Figure 2 shows the November 20, 2003 storm in a similar fashion. This time, only the eastern half of the U.S. is shown. The big feature appears different than what was seen previously (i.e., it has a distinctive "finger-shape" in it), and it seems to move faster. However, additional sharp gradients between dark red and blue zone are observed. These sharp transition areas are the focus in this study since they are likely to have the highest spatial gradients.

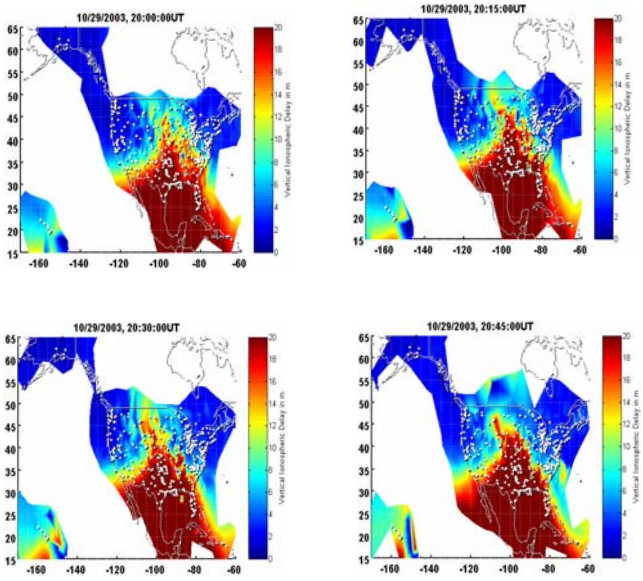

Figure 1: Ionosphere Spatial Anomalies Observed during October 29, 2003 Storm

As described in our previous work (see [3,4,5]), ionosphere anomalies are modeled as wave fronts in order to study their impact on a LAAS user. Figure 3 illustrates this simplified model. The gradient represents a linear change in vertical ionosphere delay between the "high" and "low" delay zones. Four parameters are used to characterize the anomaly: gradient slope (in mm/km), gradient width (in km), front speed (in m/s), and maximum delay (in m). Note that the total delay difference is simply the product of gradient slope and width.

Imagine an ionosphere anomaly "sweeping through" a LAAS-equipped airport (a "moving scenario"). The worst case from the aircraft's point of view is a wave

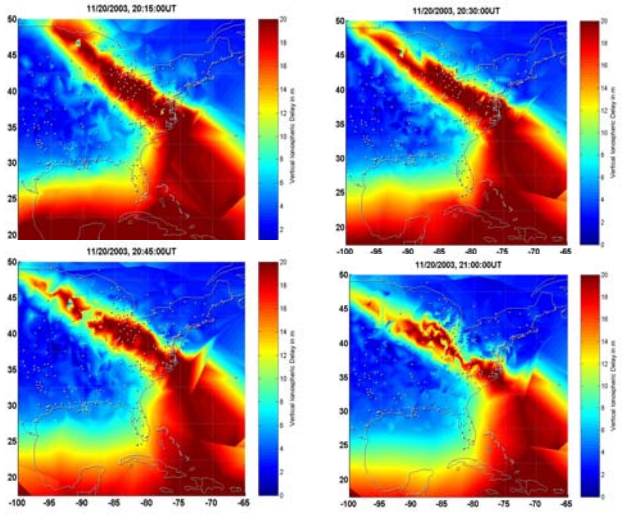

Figure 2: Ionosphere Spatial Anomalies Observed During November 20, 2003 Storm

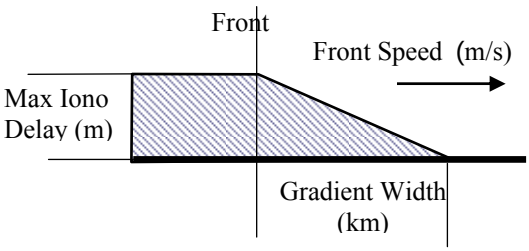

Figure 3: Simplified Model of Ionosphere Anomaly

front that approaches from directly behind an aircraft on approach and overtakes its ionosphere pierce point before the aircraft reaches its decision height. After the wave front overtakes the aircraft, a differential range error builds up as a function of the rate of overtaking and the slope of the gradient. Before the wave front reaches the corresponding LGF pierce point, there is no way for the LGF to observe (and thus be able to detect and exclude) the anomaly. The worst-case timing of this event is such that the maximum differential error occurs (often this means the time immediately before LGF detection and exclusion) at the moment when the aircraft reaches the decision height for a particular approach (the point at which the tightest vertical alert limit or VAL applies). Note that this worst-case event and timing, if it ever were to occur, would only affect one aircraft. Other aircraft on the same approach would be spread out such that the wave front passage would create no significant hazard for them, as the VAL far from the decision height is higher than the error that could result from this anomaly [7,8].

A "near-worst-case" scenario of this sort is sketched in Figure 4. In this scenario, the user is 45 km away (the limit of LAAS VHF data broadcast coverage [8]) and is

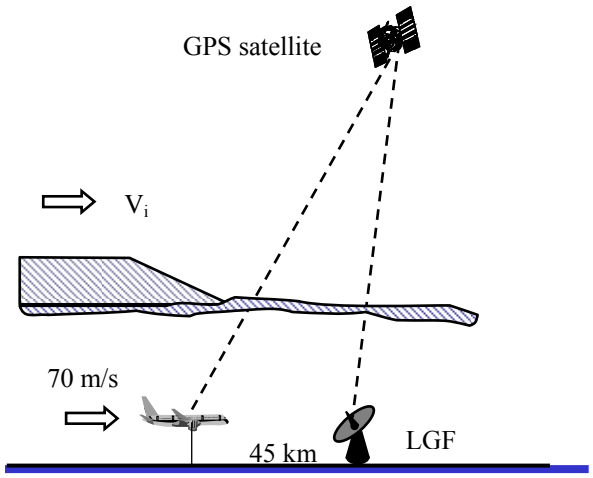

Figure 4: A "Near-Worst-Case" LAAS User Scenario

approaching the LGF at a speed of 70 m/s. The ionosphere front is behind the airplane and is moving in the same direction at a speed of V_i. The ionosphere front is going to "catch" the airplane (reach the IPP between the aircraft and the GPS satellite), pass it, and eventually hit the IPP between the LGF and the satellite. The LGF "sees" the ionosphere from then on and gradually incorporates it into its differential corrections. The impact of this ionosphere anomaly model on LAAS users was analyzed in detail in [3,4].

From ionosphere "movies" are compiled from many snapshots like those in Figure 1 and 2 for a longer period of time, it seems that most ionosphere anomalies move much faster (relative to the ground) than an approaching airplane. This is not surprising, as the ionosphere is expected to move with the solar-magnetic frame, which is moving relative to the ground at a speed that is significantly faster than an approaching airplane (70 m/s). To be conservative, another category has been created to cover "stationary scenarios", which means that the front stays still or moves slower than the approaching airplane. Note that this scenario is potentially more threatening to LAAS users since, if the front stops moving before reaching the LGF, then there is no way that the LGF can detect it! Therefore the error could grow larger without being detected, and multiple aircraft can be affected depending on how long the front "dwells" in one place.

Based on previous data studies [2,3,5], the spatial threat model accepted by the FAA/RTCA LAAS ionosphere anomaly working group in September 2004 is reviewed here as Table 1 [18]. This model is divided to three sub-models: Low elevation angle (El $\leq$ 12°), high elevation with moving front (1000 m/s > front speed > 70 m/s), and high elevation with "stationary" front (front speed $\leq$ 70 m/s). The maximum slopes are set to be 150 mm/km, 500 mm/km, and 250 mm/km, respectively. For all three sub-models, the gradient width ranges between 25 – 200 km, and the "maximum delay difference" constraint is set to be 25 m. Previous worst-case analysis showed that the existing (single-frequency) LAAS architecture appears vulnerable to ionosphere spatial gradients at the extremes of this threat model, particularly near-stationary gradients of 250 mm/km in vertical [3].

Table 1: Ionosphere Threat Model Revised in Sept. 04

Elevation	Speed	Width	Slope	Max Error
Low elevation < 12°	0 – 1000 m/s	25 – 200 km	30 – 150 Mm/km	25 m
High elevation ≥ 12°	70 – 1000 m/s	25 – 200 km	30 – 500 mm/km	25 m
	0 –70 m/s	25 – 200 km	30 – 250 mm/km	25 m

2.0 DATA ANALYSIS

2.1 Methodology

Although WAAS "supertruth" data provides a credible indicator of an ionosphere anomaly, the limited number of reference stations (25 over CONUS) makes it hard to study those events in detail. Instead, the denser IGS/CORS database is used to study those anomalies. Since there are more than 750 CORS stations over CONUS, smaller-scale examination of the characteristics of those storms is possible.

Ionosphere observations from "clusters" of nearby receivers are most useful, as they most closely resemble

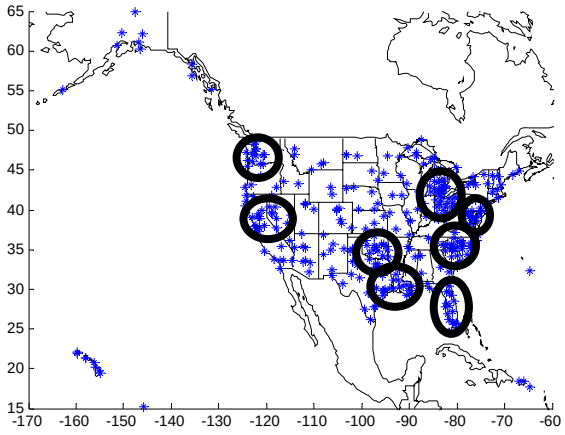

Figure 5: CORS Station Clusters in CONUS

LAAS baselines and minimize the extrapolations needed from the "thin-shell" model of the ionosphere, which is known to be erroneous during ionosphere storms (see [17]). Figure 5 shows eight IGS/CORS "clusters" identified within CONUS. Each cluster contains 10 – 30 receiver stations with separations of 25 – 200 km. For each pair of stations looking at the same satellite, their lines-of-sight are almost parallel to each other; thus the error caused by the thin-shell model is minimized. For the same reason, station separation is used instead of ionosphere pierce point (IPP) separation to estimate the gradient slope.

JPL-processed dual frequency ionosphere estimates [9] are used to calculate differential ionosphere delays between the two stations. The gradient slope is estimated as the ionosphere differential delay divided by the station separation. Since the L2 measurements have occasional outages or "jumps" due to the limited margin inherent in codeless or semi-codeless L2 tracking, the resulting ionosphere delay estimation may be erroneous. Therefore, we use L1 measurements (only) from the raw CORS data (prior to JPL post-processing) to validate the dual-frequency estimates. For the single-frequency estimate, we use L1 code (pseudorange) minus L1 carrier (phase) and divide the difference by two due to the dispersive impact of ionosphere delay on code and carrier measurements. A comprehensive methodology for ionosphere anomaly data assessment was developed to automatically search for anomalies and speeds within the Conterminous United States (CONUS) region during days of severe ionosphere activity, also known as "ionosphere storm days". Because the measurements of ionosphere delay come from imperfect receivers whose ability to track GPS signals is also affected by severe ionosphere behavior, each apparent anomaly must be examined in order to determine whether it is caused by a real ionosphere event or, instead, results from faulty measurements. The detailed description of data analysis process can be found in [15].

2.2 Ohio/Michigan (OH/MI) Cluster Re-examination

Previous data studies have demonstrated that most identifiable ionosphere anomalies moved reasonably fast (i.e., much faster than 70 m/s). The few events that appeared to be "stationary" at the beginning could not be validated after thorough investigation. According to previous threat analysis [3,4], the "stationary front" scenario remains threatening since the LGF may never be able to observe it (e.g., if the ionosphere front stops moving at the worst possible location prior to reaching the LGF). Thus, it is important to determine, to the extent possible, if a stationary or slow-moving ionosphere anomaly can be shown to exist within the database of

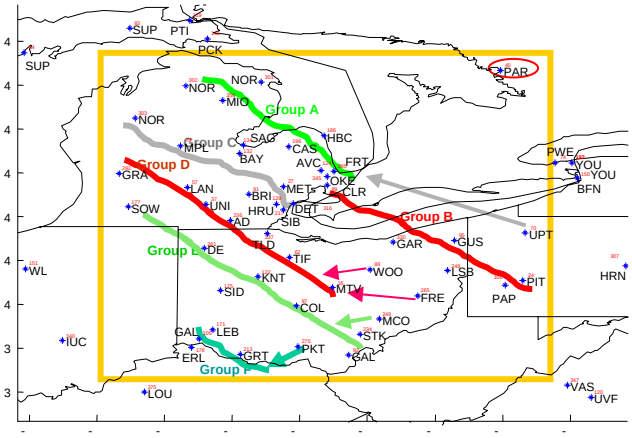

Figure 6: CORS Stations in OH/MI Region

ionosphere storm days available to us, and if so, how severe it is in terms of spatial gradient slope.

CORS data from the OH/MI cluster has been re-examined for this purpose. Figure 6 shows the stations included in the cluster. Lines indicate groupings of stations used in our analysis. As an example, ionosphere delays observed on SVN 38 at stations from Groups B and D were plotted in Figure 7. Here, the *x*-axis is the GPS time in 10 minute intervals (the traces last about 350 minutes), and the *y*-axis represents slant delay in meters. In this plot, all traces follow each other closely, which indicates that a very similar anomaly front crossed those stations one after another. Note that it is hard to estimate the gradient width and front speed because a fast moving, wide front would appear the same (from the point-of-view of two nearby IGS/CORS stations) as a slow-moving, narrow front. Under the assumption that the same front crosses multiple stations without changing direction or speed, it is possible to estimate the speed and width if multiple nearby stations are present.

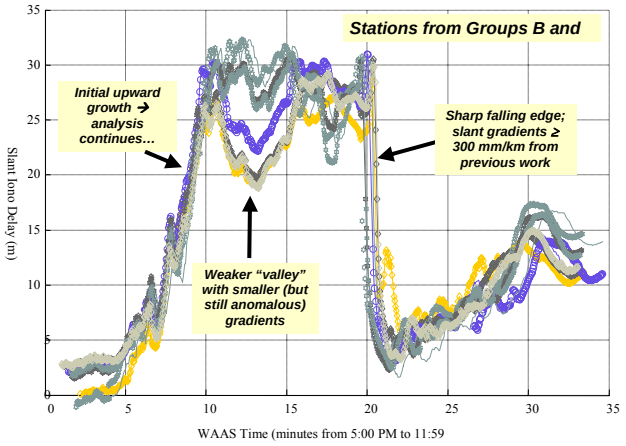

Figure 7: Ionosphere Delay Observed at Various Stations (Groups B and D) in OH/MI Cluster

As can be seen in Figure 7, the ionosphere delay increased from near zero to about 30 meters in the first 100 minutes. Then several smaller-scale variations occurred during the period from 100 to 200 minutes. This was followed by an extremely sharp fall where the delay dropped about 25 meters in 10 minutes. From 200 minutes on, the delays increased slowly until SVN 38 set. A gradient of more than 300 mm/km was found during this sharp falling edge in previous work. Three stations were used to estimate the speed associated with that particular example, and it was found to be about 250 mm/km [15] (also see [10]). Since many more stations were used in this study, more speed estimation data points were obtained. The histogram of speed estimation around the sharp falling edge is shown as Figure 8. It indicates that most of the apparent speeds are around 300 – 400 m/s. A few points lower than 100 m/s do exist, but further investigation indicates that those results came from stations that are far apart, which makes the basic assumption (same front feature across various stations) less solid. Figure 9 is the histogram corresponding to the "valley" part of the traces, i.e., the period between 100 to 200 minutes in Figure 7. While work is ongoing to investigate the rising edge period in the first 100 minutes, we have concluded that no slow-moving anomaly has been found with sufficient confidence.

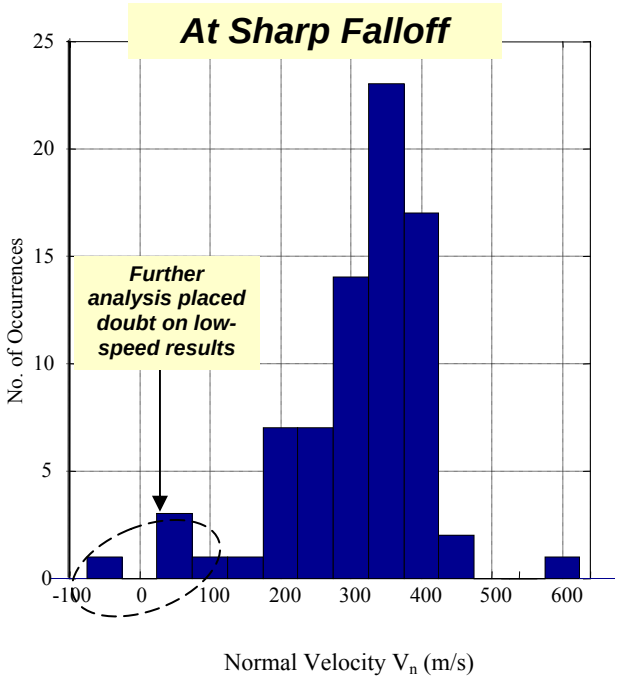

Figure 8: Histogram of Slant Gradients Observed in OH/MI on 11/20/03 (*Falling Edge*)

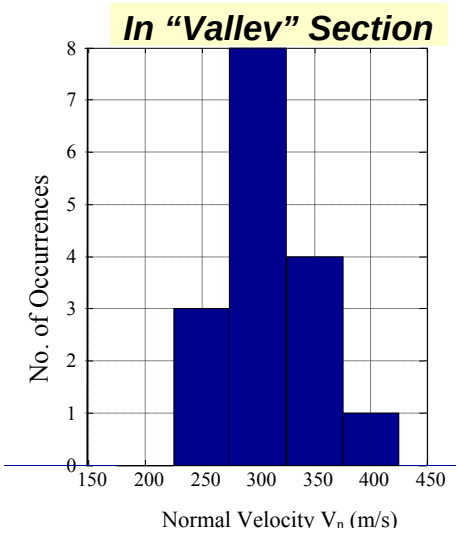

Figure 9: Histogram of Slant Gradients Observed at OH/MI on 11/20/03 (*"Valley" Period*)

2.3 Florida Data

In addition to the large scale ionosphere "wall" observed on October 30, 2003, as indicated in Figure 1, another related but distinct feature occurred in Florida region in the early hours (UT) on October 31, 2003. The so-called "Florida feature" seen the previous day appeared to be smaller in scale and less significant in delay but persisted longer in time [14]. Figure 10 shows snapshots of the ionosphere movie from 1:00 to 6:40 AM (UT) on October 31, 2003, with an interval of 20 minutes. In those plots, the *x*-axis is longitude, and the *y*-axis is latitude. The color shading represents vertical ionosphere delay with dark red as 10 m and dark blue as 1 m. Unlike previous observations, the ionosphere anomaly appeared to be a small ionosphere "bubble" hanging over Florida region without rapid motion. It seemed to be "stationary" or slow-moving for a couple of hours before gradually disappeared after 5 AM.

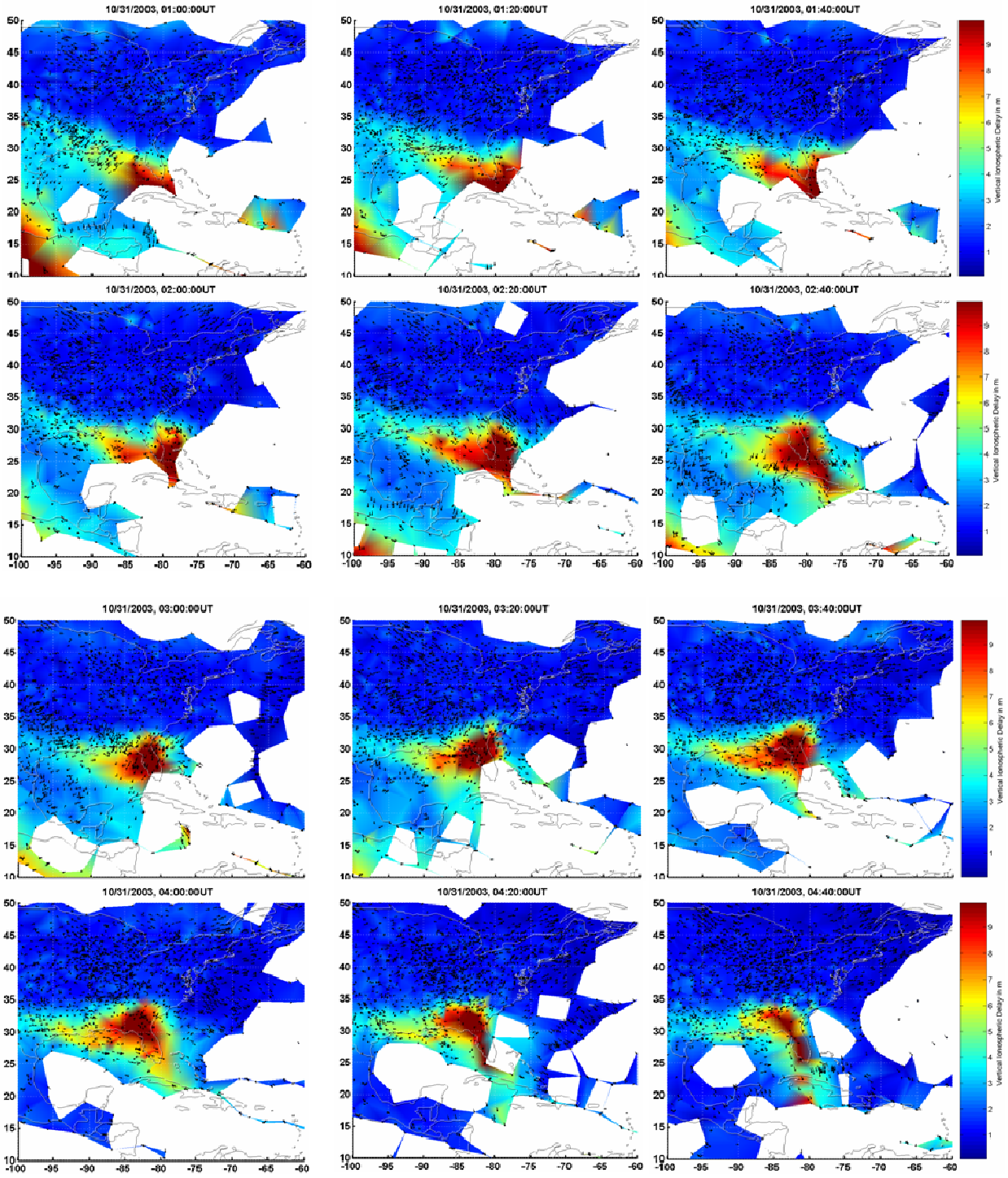
10/31/2003, 01:00:00UT
10/31/2003, 01:20:00UT
10/31/2003, 01:40:00UT
10/31/2003, 02:00:00UT
10/31/2003, 02:20:00UT
10/31/2003, 02:40:00UT
10/31/2003, 03:00:00UT
10/31/2003, 03:20:00UT
10/31/2003, 03:40:00UT
10/31/2003, 04:00:00UT
10/31/2003, 04:20:00UT
10/31/2003, 04:40:00UT
Vertical Ionospheric Delay in m

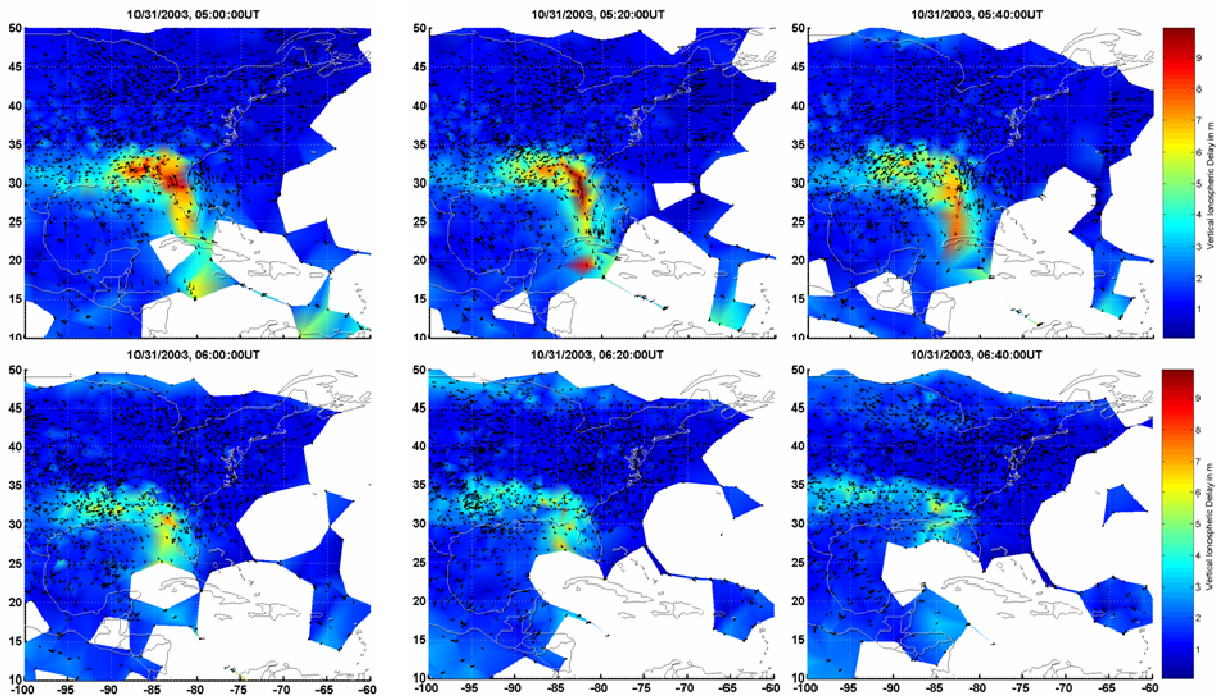

Figure 10: Ionosphere Anomaly "Snapshots" around Florida on 10/31/03

In order to further investigate this "Florida feature," CORS data from Florida region was examined carefully. The CORS station map for the region is shown in Figure 11. As before, dual frequency estimation based on JPL-processed data and L1-only estimation based on raw CORS data were both conducted and compared. Only stations in the three circles (NE, NW, and SW Florida) were used in single-frequency ionosphere estimation.

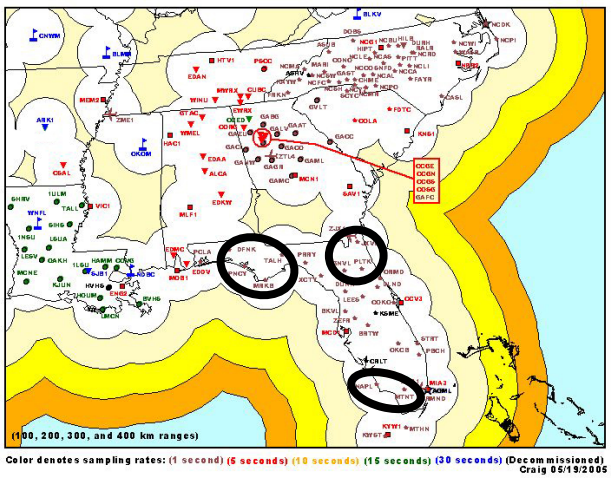

Figure 11: CORS Stations in Florida Region

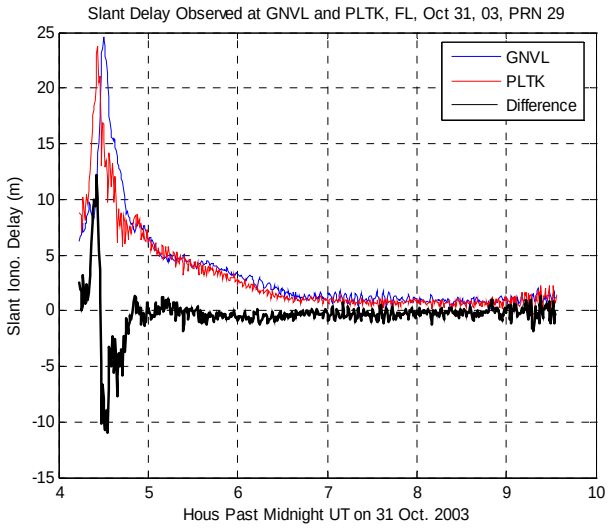

Figure 12: Slant Ionosphere Delay for PRN 29 observed at CORS Stations GNVL and PLTK

Figure 12 shows a strong gradient on PRN (and SVN) 29 observed at CORS stations GNVL (Gainesville) and PLTK (Palatka). The *x*-axis represents hours past midnight UT on 31 October 31, 2003. The *y*-axis is slant ionosphere delay in meter estimated by the L1 code-minus-carrier technique. The delay at GNVL is plotted in red, while the delay at PLTK is in blue. The maximum

slant delay reaches about 25 meters, which is well beyond the normal range. The two curves follow each other closely with the red being "ahead of" the blue for about 4 minutes, which indicates that the two stations probably observed the same anomaly, with PLTK seeing it about 4 minutes earlier that GNVL did. Since differential error matters the most from a LAAS user's point of view, a black trace is drawn in the same plot to show the difference observed from the two stations. The peak differential delay is about 12 meters. Note that the two stations are about 60 km apart, with GNVL being almost due west of PLTK. The slant spatial gradient along the line between these two stations can be estimated as 12 m / 57 km = 210 mm/km. SV 29 was low in the sky with elevation angle about 12 - 15° at that time. Taking the obliquity factor into account, if the thin-shell model were valid for this event, the vertical gradient would be about 80 mm/km.

The velocity of the ionosphere anomaly traveling between GNVL and PLTK can also be estimated. The observed speed is due to the combination of ionosphere anomaly and satellite motion. After removing the satellite motion (in this case, the IPP was moving about 143 m/s from south to north with an angle of 6° from the north), the speed of ionosphere anomaly moving between PLTK to GNVL is estimated to be 220 m/s. Note that this is the speed projected to the direction of the line between PLTK and GNVL; the normal velocity (perpendicular to the ionosphere "front") may be faster. Because it is a fast-moving event, as stated earlier, it is less threatening to LAAS users. Although the anomaly looks "stationary" at the macro scale shown in Figure 10, closer inspection shows that, like all of the verified OH/MI cases, this particular event falls into the fast-moving category.

Figure 13 shows another example with the same two stations but a different satellite, PRN 10 (SVN 40). It is also based on L1 code-minus-carrier estimation. In this case, the maximum differential slant delay reached 5.7 m at about 04:40 UT on October 31, 2003. The corresponding slant gradient was about 100 mm/km. Since PRN 10 was high on the sky with an elevation angle of 70 – 80°, the vertical gradient delay was also about 100 mm/km. Note again that the gradient estimated using this method is actually the projection of the normal gradient to the direction of the line between the two stations. Therefore the normal gradient could be larger depending on the angle between the ionosphere "front" and the line between GNVL and PLTK. Similarly, the velocity of the ionosphere anomaly traveling from PLTK to GNVL can be estimated. It appeared to take about 16 minutes for the ionosphere peak event to move from PLTK to GNVL. After removing the known satellite motion, the "front" speed was estimated to be about 65 m/s. Again, this is the speed projected to the direction of the line between PLTK and GNVL; the normal velocity (perpendicular to the ionosphere "front") may be faster. Recall that, since the "dividing line" between "slow" and "fast" was set to be 70 m/s in the threat model (the airplane speed during approach was assumed to be 70 m/s), this example appears to fall into the "slow-moving" category.

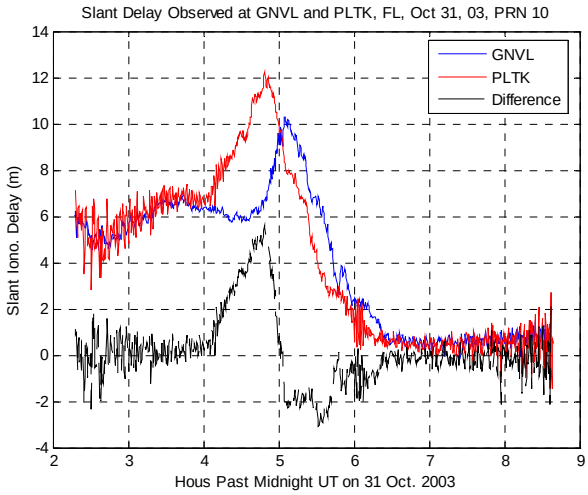

Figure 13: Slant Ionosphere Delay for PRN 10 observed at CORS Stations GNVL and PLTK

As explained in previous work (see [15]), there is an ambiguity in removing the absolute-ionosphere-delay bias from L1 code-minus-carrier data. The resulting gradient estimation inherits this uncertainty. Because dual-frequency based ionosphere delay estimation observes absolute (as well as relative) ionosphere delay, it does not suffer the same problem. However, because semi-codeless L2 tracking is not as robust as L1 tracking, normally the dual-frequency data from CORS stations experiences more data loss then the L1-only case. As a result, the two methods are complementary to each other. Figure 14 shows the dual-frequency results for the same stations and satellite as in Figure 13. The two methods produce the same estimates for gradient and speed and thus agree with each other very well.

The next step is to check if other stations in Florida observed similar events. Instead of GNVL and PLTK (which are at about the same latitude), JXVL (Jacksonville) is selected to form a pair with PLTK (the two are about the same longitude and this form a North-South baseline about 75 km long). Figure 15 shows L1 code-minus-carrier data for PRN 10. A similar ionosphere anomaly was observed between PLTK and JXVL. Along the direction of JXVL to PLTK, the estimated gradient was about 80 mm/km and the velocity was around 135 mm/km. Since the gradient is smaller while the speed is faster, LAAS user aircraft moving in a North-South direction would not have experienced as threatening an ionosphere anomaly.

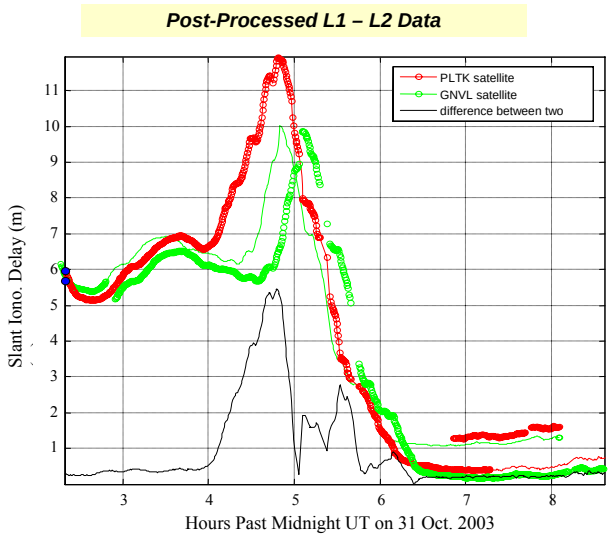

Figure 14: Dual-Freq. Slant Ionosphere Delay for PRN 10 observed at CORS Stations GNVL and PLTK

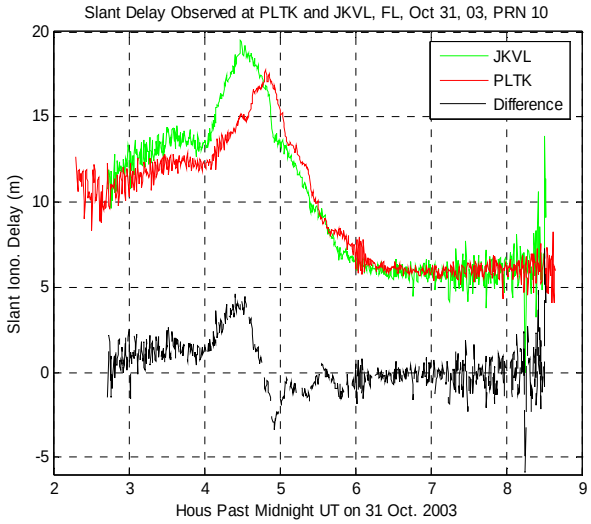

Figure 15: Slant Ionosphere Delay for PRN 10 observed at CORS Stations JXVL and PLTK

Figure 16 shows L1 code-minus-carrier data for PRN 10 obtained from CORS stations NAPL (Naples) and MTNT (West of Miami). Those stations are in southwest Florida and are about 400 km away from station GNVL, with NAPL being WNW of MTNT. A slow-moving pattern similar to the one seen from NE Florida is also observed. In this case, the peak differential slant delay was about 7 meters. The slant (and vertical) spatial gradient alone the line of these two stations are estimated to be 100 mm/km. It appears to take about 25 minutes for the ionosphere anomaly to travel from MTNT to NAPL. After removing the SV motion, the ionosphere front velocity from MTNT to NAPL is estimated to be about 40 m/s. Again, these estimates give only the projection along the line between these two stations – the gradient and velocity normal to the front may be higher.

Figure 17 shows the ionosphere delay observed for PRN 10 from all stations that are available from the dual-frequency process. As can be seen, all of these traces follow each other reasonably well. In addition, this composite plot demonstrates that the approximately ENE-to-WSW motion of the PRN 10 event (along with the gradual decrease in the peak ionosphere delay) is consistent across these stations. Taken together, these results strongly suggest that that this ionosphere event is real; thus slow-moving ionosphere anomalies should be included in the LAAS ionosphere anomaly threat model.

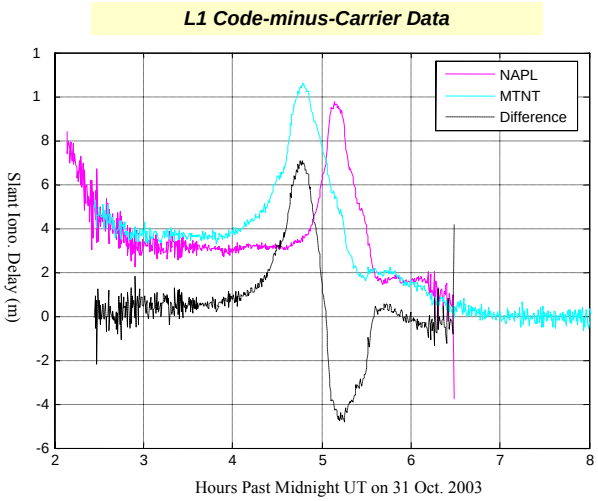

Figure 16: Slant Ionosphere Delay for PRN 10 observed at CORS Stations NAPL and MTNT

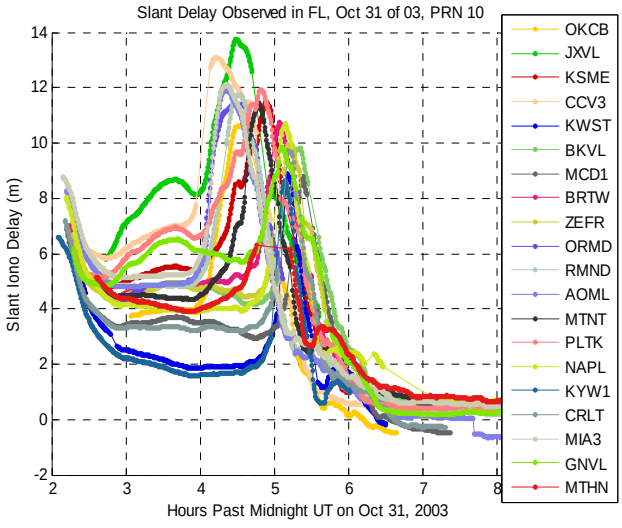

Figure 17: Slant Ionosphere Delay for PRN 10 observed at Multiple CORS Stations

3.0 LAAS IMPACT ANALYSIS

3.1 LAAS Availability Assessment

In order to examine the impact of ionosphere anomalies on LAAS users based on the September 2004 threat model shown in Table 1, a simulation was performed for Memphis Airport, which will be the site of the LAAS "Provably Safe Prototype" or PSP. Instead of the RTCA-standard 24-satellite constellation, a recent constellation almanac (the one for July 18, 2005) was used. A total of 145 geometries were considered to cover one repeatable day at 10-minute intervals. Figure 18 shows the results under the assumption that all satellites indicated as "healthy" in the 7/18/05 almanac are in fact usable. The *x*-axis is the geometry index, and the *y*-axis is vertical error in meters. Blue stars represent simulated vertical errors caused by combinations of specific ionosphere anomaly parameters within the threat space. The red curve represents a typical LAAS user value for VPL_{H0} for each geometry (see [16]). In this scenario, no geometry has a maximum ionosphere-induced vertical error greater than 10 meters, which is the current Vertical Alert Limit or VAL for LAAS CAT I precision approaches. The maximum VPL_{H0} among these geometries is about 5 meters. Note that the maximum error exceeds VPL_{H0} for all geometries.

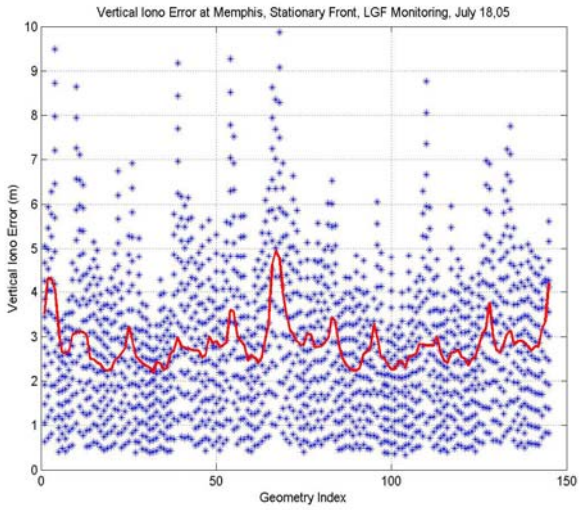

Figure 18: Availability Assessment for Stationary Fronts at Memphis PSP Site (*All SVs Healthy*)

While not necessarily present on 7/18/05, satellite outages occur from time to time due to satellite failures and scheduled maintenance. Figure 19 shows the resulting availability for all possible one-SV-out cases, meaning that every geometry in time was simulated with each one of its visible satellites presumed to be unavailable; thus creating many more possible satellite geometries. All other conditions are the same as in Figure 18. As expected, with one satellite out, vertical errors are significantly greater than the previous case -- the maximum error over all geometries increases to 22 meters. There are 46 geometries (out of 4060) that have maximum ionosphere error exceeding the Vertical Alert Limit (VAL) of 10 meters. Those geometries have to be excluded to protect the safety of LAAS CAT I users, and this would result in an availability loss of 0.0113. Note that this simulation provides an ideal performance ceiling, although it is not practical in real time because there is no way to precisely determine which geometries are acceptable and which are not. In order to protect LAAS user integrity under this ionosphere threat, conservative geometry screening methods could be used, but they would eliminate many otherwise-usable geometries and thus lead to much greater availability loss.

In addition to analyzing data in order to validate or revise the parameters of the ionosphere threat model, it is also instructive to study LAAS availability sensitivity to these parameters. Since the unsuitability of the thin-shell model during anomalous ionosphere conditions is now well-understood, and because the vertical threat-model parameter bounds in Table 1 bound all validated anomaly observations in slant as well, it has been proposed to specify gradients in an updated threat model in the slant domain instead of in the vertical one. If the threat model were changed such that the maximum slant gradient is 200 mm/km for stationary/slow-moving scenarios, then the resulting availability is shown in Figure 20. The same one-SV-out geometries used in Figure 19 are used here, but the significant reduction in the stationary/slow-moving component of the threat space (from an upper bound of 250 mm/km in vertical to 200 mm/km in slant)

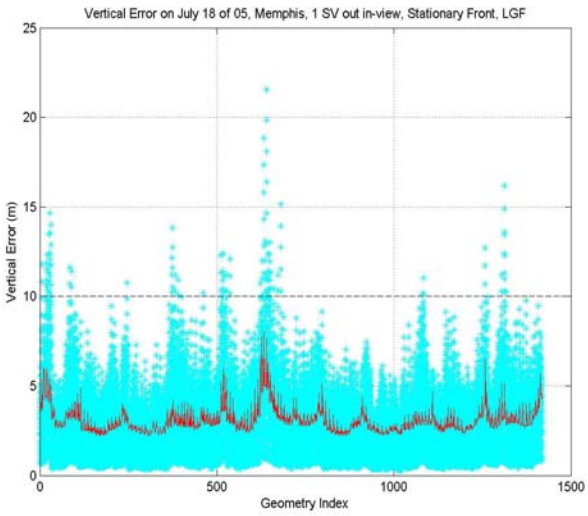

Figure 19: Availability for Stationary Fronts at Memphis PSP Site (*One SV Unhealthy*)

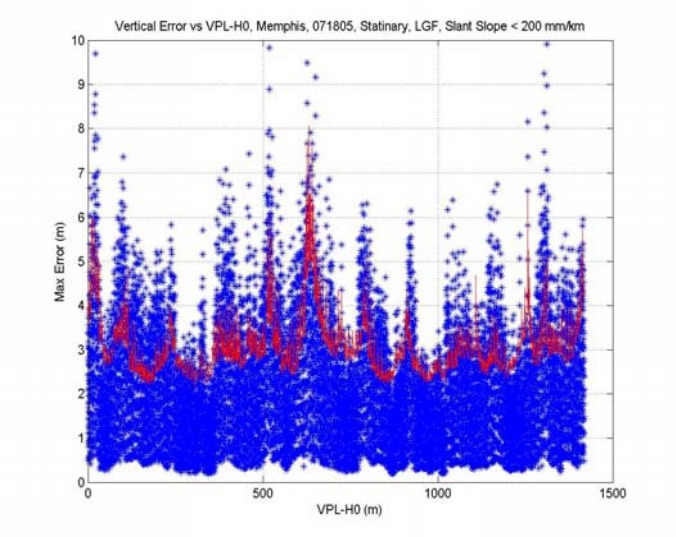

Figure 20: Availability for Stationary Fronts at Memphis PSP Site (*One SV Unhealthy; Slant Gradient ≤ 200 mm/km*)

results in all vertical user errors induced by ionosphere anomalies being below the 10-meter CAT I VAL. Thus, there would be no availability loss caused by such anomalies if bounding maximum ionosphere-induced errors by VAL were sufficient to insure safety. If a stricter standard that VPL_{H0} must bound the maximum ionosphere error were enforced, some availability loss would occur, but the needed inflation of VPL_{H0} to bound all blue points in Figure 20 is possible without a major loss of CAT I LAAS availability (partially because VPLH0 in a fielded system will exceed the ideal curve shown here for other reasons as well). This is not at all the case in Figure 19.

Clearly, the potential impact of ionosphere anomalies on LAAS users is extremely sensitive to the maximum spatial gradient in the stationary/slow-moving component of the ionosphere threat model. Fortunately, the slow-moving examples we have found from the Florida data thus far (all of which are part of a single event) support this reduced threat model. If no other slow-moving events with gradients above 100 mm/km in slant are found in the remaining OH/MI or Florida data, it may be possible to reduce this upper bound from the 200 mm/km assumed in Figure 20 to as low as 125 mm/km (leaving some margin for measurement uncertainty). If this occurs, the impact of slow-moving or stationary ionosphere anomalies on CAT I LAAS availability will be minimal.

3.2 Data-Replay Analysis (or "End-Around Check")

In previous work (see [19]), an "end-around check" was performed to demonstrate that the results obtained by simulation of ionosphere anomalies as linear wave fronts can reasonably approximate the result that is achieved by using observed data between two points, treating one as a (static) LAAS user and one as a LAAS reference station. The procedure for this "data-replay analysis" is as follows:

1) Assign the stations within a station pair (used to estimate threat-model parameters) such that the station impacted first by a severe gradient is treated as a stationary LAAS pseudo-user and the other station is treated as the LGF;

2) Subtract "LGF" measurements from "user" measurements and obtain the "observed" differential ionosphere delay between the two stations;

3) "Pad" the data as needed to implement standard LAAS carrier-smoothing filters with a 100-sec time constant;

4) Combine the "observed smoothed user pseudorange error" with the GPS satellites visible and usable at the time the observations were made to compute the resulting vertical position error.

In addition to validating simulation results, this "data-replay" approach provides a different viewpoint on LAAS vulnerability because it is limited to events that actually occurred as opposed to worst-case extrapolations of threat-model parameters gleaned from these events.

Figure 21 shows an example of such a "data-replay" analysis for the "slow-moving" GNVL/PLTK anomaly on PRN 10 reported in Section 2.3. This analysis pretends that the LGF is located at GNVL and a static LAAS user is at PLTK (recall that PLTK is East of GNVL and is impacted first – see Figure 13). Differential range errors for each usable satellite are shown in the plot. The largest range error is on PRN 29, which is the fast-moving large gradient (about 210 mm/km in slant) shown in Figure 12.

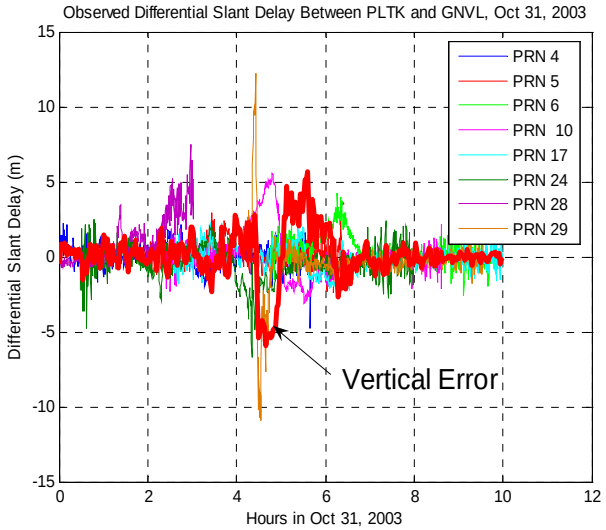

Figure 21: Data-Replay Analysis for GNVL/PLTK

Because the ionosphere anomaly affecting PRN 29 is moving quickly, it reaches GNVL soon after passing PLTK and would be detected (causing PRN 29 to be excluded from use) by an LGF located at GNVL. The slow-moving ionosphere anomaly on PRN 10 causes a smaller differential range error, but it is interesting to see that the PLTK user's vertical position error (estimated based on the known GPS satellite almanac for 10/31/03), which is shown by the thick red line, reaches its maximum of just over 5 meters at about the same time as the PRN 10 range error reaches its maximum. Thus, the PRN 10 event likely is the most significant cause of the 5-meter peak vertical error at PLTK.

In judging the significance of this result, it must be remembered that GNVL and PLTK are about 60 km apart, which is much further than the effective LAAS user-to-LGF separation at the CAT I decision height (which, including the lag caused by 100 seconds of smoothing, is no more than 20 – 25 km). Thus, the actual differential error suffered by a LAAS user approaching GNVL during this event would be significantly smaller (the anomaly simulation tool can be used to determine how much smaller). Given this fact, it is clear that this event does not pose a significant hazard to LAAS users.

4.0 CONCLUSIONS AND FUTURE WORK

In this study, the existing CORS database from the OH/MI cluster on 11/20/03 was revisited, and observations from Florida region on 10/31/03 (UT) have been studied to examine the credibility of stationary or slow-speed ionosphere anomalies. While no clear slow-speed event has been discovered in the OH/MI data, at least one verifiable slow-speed event has been discovered. This event on a high-elevation satellite (PRN 10) has been confirmed by multiple CORS stations and station pairs spread around Florida. The slopes of this one verifiable slow-moving event are as large as 100 mm/km in slant. Fortunately, gradients of this size are unlikely to be hazardous to LAAS. In contrast, while the worst OH/MI events (and the PRN 29 event in Florida) have more severe gradients, all verified points analyzed to date are moving faster than 140 m/s. Based on these results, we believe that slow-speed events should remain in the LAAS ionosphere anomaly threat model, but a significant reduction of the maximum gradient is advisable. The impact of slow-speed gradients on LAAS availability (of integrity) is not severe if the maximum slow-speed slant slope is below 200 mm/km, at the impact is likely negligible below 125 mm/km. Finally, an "end-around-check" data replay for the PLTK and GNVL stations in Florida shows that the worst-case position error is well below the 10-meter CAT I VAL and may be "boundable" by a moderately-inflated VPL_{H0}.

One component of our ongoing work on ionosphere anomaly impacts on LAAS is to complete the analysis of OH/MI on 11/20/03 and Florida on 10/31/03 to confirm that all events of significance to LAAS have been accounted for. The primary focus in the near future will be on better estimation of ionosphere front speed from this data. The other key component is to apply the "data-replay analysis" technique to the set of severe ionosphere anomalies that have been validated (or "almost-validated"). The objective of this work is to complement the results of worst-case simulations and provide a more-realistic depiction of the impact of specific validated ionosphere anomalies on LAAS users.

ACKNOWLEDGMENTS

The authors would like to thank the FAA LAAS Program Office (AND-710) for its support of this research. In addition, the help of the many participants in the LAAS ionosphere anomaly working group (including Mats Brenner of Honeywell, Tom Dehel of the FAA Technical Center, Barbara Clark of FAA aircraft certification, Ron Braff and Curt Shively of MITRE, Tim Murphy of Boeing, and Joel Wichgers of Rockwell-Collins) was of great value in completing this research. We would also like to extend our thanks to Attila Komjathy of JPL for providing processed ionosphere data. The opinions expressed here are those of the authors and do not necessarily represent those of the FAA or other affiliated agencies.

REFERENCES

[1] S. Datta-Barua, *et al*, "Using WAAS Ionospheric Data to Estimate LAAS Short Baseline Gradients," *Proceedings of ION 2002 National Technical Meeting*. Anaheim, CA., January 28-30, 2002, pp. 523-530.

[2] T. Dehel, "Ionospheric Wall Observations," Atlantic City, N.J., William J. Hughes FAA Technical Center, FAA ACT-360, February 24, 2003.

[3] M. Luo, , *et al*, "Ionosphere Threat to LAAS: Updated Model, User Impact, and Mitigations", *Proceedings of ION GNSS 2004*, Long Beach, CA.., Sept. 21-24, 2004.

[4] M. Luo, *et al*, "LAAS Ionosphere Spatial Gradient Threat Model and Impact of LGF and Airborne Monitoring," *Proceedings of ION GPS 2003*, Portland, OR., Sept. 9-12, 2003.

[5] M. Luo, *et al*, "Ionosphere Spatial Gradient Threat for LAAS: Mitigation and Tolerable Threat Space", *Proceedings of ION 2004 Annual Meeting*, San Diego, CA., Jan 26-28, 2004.

[6] P. Misra, P. Enge, *Global Positioning System: Signals, Measurements, and Performance, 2nd Ed.*. Lincoln, MA., Ganga-Jamuna Press, 2004.

[7] *Minimum Aviation System Performance Standards for Local Area Augmentation System (LAAS).* Washington, D.C., RTCA SC-159, WG-4A, DO-245, Sept. 28, 1998.

[8] *Specification: Performance Type One Local Area Augmentation System Ground Facility.* Washington, D.C., Federal Aviation Administration, FAA-E-2937A, April 17, 2002.

[9] A. Komjathy, *et al*, "The Ionospheric Impact of the October 2003 Storm Event on WAAS," *Proceedings of ION GPS 2004*, Long Beach, CA., Sept. 21-24, 2004.

[10] T. Dehel, *et al*, "Satellite Navigation vs. the ionosphere: Where Are We, and Where Are We Going?", *Proceedings of ION GPS 2004*, Long Beach, California., Sept. 21-24, 2004.

[11] G. Xie, *et al*, "Integrity Design and Updated Test Results for the Stanford LAAS Integrity Monitor Testbed (IMT)," *Proceedings of ION 2001 Annual Meeting*. Albuquerque, NM., June 11-13, 2001, pp. 681-693.

[12] B. Pervan, "A Review of LGF Code-Carrier Divergence Issues", Illinois Institute of Technology, MMAE Dept., May 29, 2001.

[13] G. Xie, *et al*, "Detecting Ionospheric Gradients with the Cumulative Sum (CUSUM) Method," Paper AIAA 2003-2415, *Proceedings of 21st International Communications Satellite Systems Conference*, Yokohama, Japan, April 16-19, 2003.

[14] S. Datta-Barua, *et al*, "Verification Of Low Latitude Ionosphere Effects on WAAS During October 2003 Geomagnetic Storm," *Proceedings of ION Annual Meeting 2005*, Cambridge, MA., June 27-29 2005.

[15] A. Ene, D. Qiu, *et al*, "A Comprehensive Ionosphere Storm Data Analysis Method to Support LAAS Threat Model Development," *Proceedings of ION Technical Meeting 2005*, San Diego, January 15-20, 2005.

[16] *Minimum Operational Performance Standards for GPS/Local Area Augmentation System Airborne Equipment*. Washington, D.C., RTCA SC-159, WG-4A, DO-253A, Nov. 28, 2001.

[17] S. Pullen, *et al*, "Plan for CAT I LAAS Ionosphere Anomaly Resolution," RTCA SC-159 WG-4 Meeting, Seattle, WA., July 28, 2004.

[18] S. Pullen, *et al*, "Status of CAT I LAAS Ionosphere Anomaly Resolution," RTCA SC-159 WG-4 Meeting, Washington, D.C.., Oct. 5, 2004

[19] M. Luo, "End-around-Check with LGF Monitor," Stanford University, May 3, 2005.